

The influence of microstructures and crystalline defects on the superconductivity of MgB₂

A. Serquis, X. Y. Liao, Y. T. Zhu, J. Y. Coulter, J. Y. Huang, J. O. Willis,

D. E. Peterson, and F. M. Mueller

Superconductivity Technology Center, MS K763, Los Alamos National Laboratory, Los Alamos, NM 87545, USA

N. O. Moreno and J. D. Thompson

Condensed Matter and Thermal Physics, MS K764, Los Alamos National Laboratory, Los Alamos, NM 87545, USA

S. S. Indrakanti and V. F. Nesterenko

Department of Mechanical and Aerospace Engineering, University of California, San Diego, La Jolla, CA 92093

This work studies the influence of microstructures and crystalline defects on the superconductivity of MgB₂, with the objective to improve its flux pinning. A MgB₂ sample pellet that was hot isostatic pressed (HIPed) was found to have significantly increased critical current density (J_c) at high fields than its un-HIPed counterpart. The HIPed sample had a J_c of 10000 A/cm² in 50000 Oe (5 T) at 5K. This was 20 times higher than that of the un-HIPed sample, and the same as the best J_c reported by other research groups. Microstructures observed in scanning and transmission electron microscopy indicate that the HIP process eliminated porosity present in the MgB₂ pellet resulting in an improved intergrain connectivity. Such improvement in intergrain connectivity was believed to prevent the steep J_c drop with magnetic field H that occurred in the un-HIPed MgB₂ pellet at $H > 45000$ Oe (4.5 T) and $T = 5$ K. The HIP process was also found to disperse the MgO that existed at the grain boundaries of the un-HIPed MgB₂ pellet and to generate more dislocations in the HIPed the pellets. These dispersed MgO particles and dislocations improved flux pinning also at $H < 45000$ Oe. The HIPing process was also found to lower the resistivity at room temperature.

74.70.Ad, 74.60.Ge, 74.62.Bf, 74.25.Fy

I. INTRODUCTION

The discovery of superconductivity at 39 K in MgB₂ by Nagamatsu et al.¹ has attracted the attention of numerous researchers, especially those in applied superconductivity. One of the challenges is understanding the grain boundary properties of the MgB₂ phase: whether or not weak links are a limiting factor for intergrain critical currents, similar to the situation for polycrystalline high-T_c superconductors (HTSC). Several studies indicate that a strong intergranular current network is established in MgB₂ material, so that the current is not limited by weak-link boundaries. For example, by means of magnetization measurements of grain agglomerates, Bugolavsky et al.² have shown that within these microscopic structures, intergrain and intragrain critical currents are quite comparable in value. In addition, several authors^{3,4,5} reported that high density samples have high superconducting homogeneity and strong intergranular current flow as determined by magneto-optical studies. However, a rapid drop of the critical current (J_c) at high fields, which could be related to weak link behavior, can be seen in most studies.⁶

Several works show that the transport properties of MgB₂ are sample dependent. Both the reported resistivity at room temperature $\rho(297\text{ K})$ and the residual resistivity ratio, $\text{RRR}=\rho(297\text{ K})/\rho(40\text{ K})$ vary among different research groups by about an order of magnitude.^{1,4,7} In addition, the T_c and the J_c and its dependence on magnetic field are also sample dependent. This sample dependency has been previously attributed to the synthesis conditions (pressure or thermal history),⁸ or to the presence of Mg deficiencies or to the presence of oxygen-related defects.⁹

Several methods have been reported to obtain well-connected and dense samples, and high-pressure synthesis seems to be able to produce fully dense bulk MgB₂ with electrical transport properties superior to those of sintered samples.^{3,10} In a previous work we have produced samples with very sharp superconducting transitions using a novel Mg vapor infiltration

technique.¹¹ We have observed that Mg(O,B) precipitates provide good flux pinning in these samples leading to a J_c of 1.5×10^5 A/cm² at 5 K and 1 T,¹² which is better than that of the first works published on powders and wires.^{13,14,15} In this work we have used the hot isostatic pressing (HIPing) process to further improve flux pinning of our samples. The objective of this study is to understand the influence of the microstructures and crystalline defects produced by HIPing on the superconductivity of MgB₂.

II. EXPERIMENTAL

MgB₂ samples were synthesized using an atomic ratio of Mg:B = 1:1 at 900°C under flowing Ar. The starting materials were amorphous boron powder (-325 mesh, 99.99% Alfa Aesar) and Mg turnings (99.98% Puratronic). The boron powder was pressed to pellets (5 mm diameter x 4 mm thickness). The pellets and the Mg turnings were wrapped in Ta foil, placed in an alumina crucible inside a tube furnace under ultra-high purity flowing Ar, and heated at 900°C for two hours. We shall hereafter refer to the as-synthesized MgB₂ pellet as the un-HIPed sample. The un-HIPed sample was ground into powder and hot isostatically pressed (HIPed) at 200 MPa to form the HIPed sample. The HIPing was carried out in an ABB Mini-HIPer unit using a cycle cooling under pressure with a maximum temperature of 1000 °C, as described elsewhere.¹⁰

A SQUID magnetometer (Quantum Design) was used to measure the susceptibility of the samples over a temperature range of 5 to 45 K in an applied field of 10 Oe. Magnetization versus magnetic field (M-H) curves were measured on rectangular-shaped samples at temperatures of 5 and 30 K under magnetic fields up to 70000 Oe to determine the critical current density $J_c(H)$.

The direct current (dc) resistivity as a function of temperature was measured through the standard 4-probe method in a computer-controlled data logger system, on samples with dimensions of $\sim 2 \times 0.5 \times 0.8$ mm.

The surface morphology and microstructures of the samples were characterized using a JEOL 6300FX scanning electron microscope (SEM) and a Philips CM300 transmission electron microscope (TEM) operated at 300 kV and a JEOL 3000F TEM operating at 300 kV. TEM samples were prepared by grinding the MgB₂ pellets mechanically to a thickness of about 50 μm and then further thinning to a thickness of electron transparency using a Gatan precision ion polishing system with Ar⁺ accelerating voltage of 3.5 kV.

III. RESULTS AND DISCUSSION

Figure 1(a) shows the dc magnetization (M) as a function of temperature for the un-HIPed and HIPed samples. The magnetization of the commercial Alfa Aesar MgB₂ powder and that of the same powder HIPed from reference [7] are also shown for comparison. It is obvious that the samples synthesized in this study (both un-HIPed and HIPed) have higher T_c and sharper superconducting transitions than the as-purchased and HIPed commercial Alfa Aesar samples. It can be seen that the superconducting transition in the un-HIPed sample is slightly sharper than those of the HIPed samples. It is not clear what caused the transition broadening in the HIPed sample. However, the broadening could be related to the microstructural changes induced by the HIPing process.

As shown in Fig 1(b), if the un-HIPed sample is ground in an agate mortar resulting in particles with average size of 5-10 μm , the superconducting transition becomes broader. The same

behavior is observed if the HIPed sample is ground. The transition broadening in ground samples can be explained by the penetration length $\lambda(T)$ and its dependence on temperature, which follows the relationship:

$$\lambda(T) = \frac{\lambda(0)}{\sqrt{1-(T/T_c)^2}} \quad (1)$$

where $\lambda(0) = 110-180$ nm,^{14,15,16,17} for MgB₂. Therefore, the penetration length can be significantly larger near T_c than the particle size (leading to transition broadening) and decreases with temperature. As shown in Fig. 2 isolated particles with sizes less than 1 μm exist in the ground un-HIPed sample. These particles are smaller than the penetration length near T_c, and became superconducting at lower temperature, giving rise to the transition broadening. In other words, the transition broadening is caused by the small particle size rather than sample inhomogeneity, impurities, or weak link behavior as was suggested by Rogado et al.¹⁸

The resistivity, $\rho(T)$, of the HIPed and un-HIPed samples are shown in Fig. 3. The onset of the transition is 39.4 K for the un-HIPed sample and 38.5 K for the HIPed sample, while the transition width $\Delta T(10\% \text{ to } 90\%)$ is 0.3 K for both samples. The lower resistivity at room temperature $\rho(297 \text{ K})$ for the HIPed sample may be due to its higher density and better inter-granular connections, as will be discussed later. The $RRR = \rho(297 \text{ K})/\rho(40 \text{ K})$ of the un-HIPed and the HIPed samples are ~ 8.9 and 3.1 , respectively. Lee et. al.¹⁹ reported that single crystals of MgB₂ ($\sim 100 \mu\text{m}$) with superconducting transitions around 38.1-38.3 K and $\Delta T = 0.2-0.3$ K have an estimated resistivity at 40 K of $1 \mu\Omega\text{cm}$ and a $RRR=5$. As the phonon contribution to resistivity decreases with decreasing temperature, other defects present inside the grains (not in the grain boundaries) must have affected the resistivity near T_c. Xue et al⁹ reported a correlation between

RRR and the strain determined by Rietveld analysis of the x-ray diffraction data. In Fig. 4 we plot the strain values vs. the RRR of our samples,¹¹ together with the data of Xue et al⁹. The clear dependence of RRR upon strain confirms that the residual resistance is related to lattice distortion (strain). As we can see below, this lattice distortion may be related to the presence of higher densities of defects.

The magnetization versus magnetic field (M-H) curves of the HIPed and the un-HIPed samples is shown in Fig. 5. It can be seen from the insets that the reversible region in the HIPed sample lies above 7 T at T = 5 K and above 1.9 T at 30 K, while for the un-HIPed sample, these values are reduced to 6.2 T and 1.8 T, respectively.

$J_c(H)$ was determined using the Bean critical state model²⁰ for a long parallelepiped:

$$J_c(H)[A/cm^2] = \frac{20 \times \Delta M(H)[emu/cm^3]}{(a - \frac{a^2}{3b})[cm]} \quad (2)$$

where a and b are the lengths of the parallelepiped edges perpendicular to the magnetic field and ΔM is the width of the magnetization characteristic at the applied magnetic field H .

Figure 6 shows the dependence of J_c on the applied magnetic field for both HIPed and un-HIPed samples. The J_c at 0 T is nearly the same for both samples. However, the HIPed sample has a significantly higher J_c than the un-HIPed sample in magnetic field. The difference in J_c between the HIPed and un-HIPed samples increases with field. The un-HIPed sample shows a steep drop in J_c at higher fields ($H > 45000$ Oe and $T = 5$ K). No such steep drop in J_c is observed in the HIPed sample.

In fact, the HIPed sample has better flux pinning than samples reported earlier by other groups and is among the best reported. The excellent flux pinning in the HIPed sample was caused by the modification of microstructures and crystalline defects during the HIPing process. Therefore, it is essential to study the differences in the microstructures and defects of the HIPed and un-HIPed MgB_2 samples. Shown in Fig. 7(a) is the surface morphology of the un-HIPed sample. Well-developed grains of around 0.3-5 μm can be seen in the figure. However, the grains are not well connected on the surface. In contrast, the grains in the HIPed sample (Fig. 7(b)) are well compacted. The high density of the HIPed sample makes it possible to prepare a polished shiny surface of mirror quality (Fig. 7(c)).

Figure 8(a) shows a TEM bright-field image of the un-HIPed sample, which reveals poor connectivity among the MgB_2 grains. The white areas in the figure are pores, and the dark areas have been proven to be MgO by electron diffraction, as shown in Fig. 8(c). The MgO consists of nanometer-sized grains, as demonstrated in Fig. 8(b). The images in Figs. 7(a) and 8(a) clearly show that the MgB_2 grains of the un-HIPed sample are not well connected. In other words, weak links exist at the grain boundaries of this sample. Figure 9 shows the excellent connectivity between the MgB_2 grains of the HIPed sample. Neither pores nor MgO are seen at MgB_2 grain boundaries. The MgO , seen at the MgB_2 grain boundaries in the un-HIPed sample (Fig. 8(a)), have been broken up and dispersed inside the MgB_2 grains in the form of fine MgO particles. In addition, the dislocation density inside the MgB_2 grains is much higher in the HIPed sample (Fig. 9) than in the un-HIPed sample (Fig. 8).

In a previous work,¹² we also observed nanometer-sized coherent Mg(B,O) precipitates inside the MgB_2 grains in the un-HIPed samples, which are also present in the HIPed ones. However, because of the non-zone-axis imaging conditions used for Figs. 8(a) and 9, the

precipitates cannot be seen in these images. Note that the fine MgO particles, with sizes around 10 to 50 nm, as well as high density of dislocations, are present only in the HIPed sample. It is well known that extended defects, such as dislocation networks and small precipitates of non-superconducting second phases, are likely to be effective flux pinning centers. In other words, the higher J_c in the HIPed sample (Fig. 6) is due to effective flux pinning of finely dispersed MgO oxides particles as well as high-density dislocation networks. These finely dispersed MgO particles and high density dislocations also caused the higher strain in HIPed sample, which resulted in a low RRR value in that sample.

The steep drop in J_c at higher fields (>45000 Oe) in the un-HIPed sample is attributed to the porosity and MgO oxide on the grain boundaries. Dou et al.²¹ reported evidence for decoupling of the grains in sintered MgB₂, both through partial flux jumping and a step in the field dependence of J_c . These authors showed that initial bulk superconductor samples break down into a granular assembly beyond a certain critical value of field and temperature. As well as in our un-HIPed sample they observed a clear drop in the ΔM (which is proportional to the J_c), which can be attributed to the magnetic breakdown of the grain matrix as a result of flux penetration into the grain boundaries that may contain impurities. In the low-field region the current circulates mainly over the entire sample size (intergranular current), while in the high field region the current circulates only in the individual grains (intragranular current). It seems that for the un-HIPed sample this decoupling occurs ~ 45000 Oe at 5 K, whereas for the HIPed sample we did not observe a steep drop in the J_c up to 70000 Oe.

IV. SUMMARY

In summary, both the sample sintered at ambient pressure (un-HIPed) and the one that was HIPed present the same superconducting properties at low fields, with a very sharp transition observed by both magnetization and resistivity values. The lower RRR values can be ascribed to the presence of strain. Besides, the unHIPed sample contains discernible empty space (pores) as well as impurity phases at the grain boundaries. The weak connectivity between domains and the presence of impurities in the grain boundaries in the MgB₂ ambient temperature sintered sample seem to limit J_c at high fields, although not as severely as in high- T_c superconductors. The HIP process improves the field dependence of J_c through better connectivity of the grains, the generation of dislocations, and the destruction of MgO at MgB₂ boundaries, which is redistributed in the form of fine particles inside the MgB₂ matrix. These defects can act as effective flux pinning centers. The HIPed sample also has a higher irreversibility field, which is an important parameter in potential applications.

ACKNOWLEDGMENT

Work at Los Alamos was performed under the auspices of the US DOE Office of Energy Efficiency and Renewable Energy, as part of its Superconductivity for Electric Systems Program.

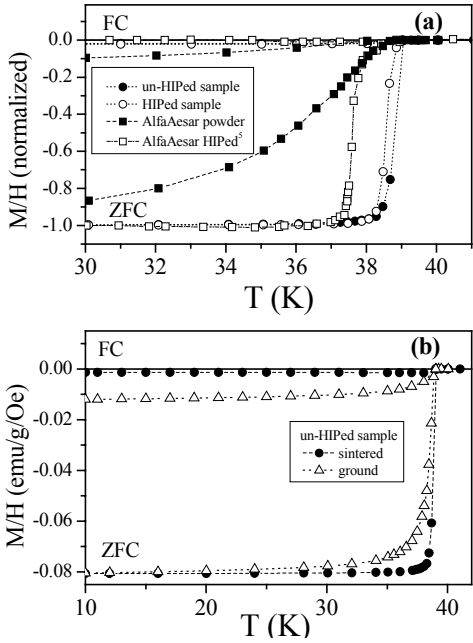


Fig. 1- (a) Magnetic susceptibility as a function of temperature of MgB₂ un-HIPed sample and the HIPed sample. For comparison we have added the data from reference [7] of the commercial Alfa Aesar MgB₂ powder and the same powder HIPed. (b) Magnetic susceptibility as a function of temperature of MgB₂, where the superconducting transition of sintered un-HIPed sample is compared with that of the same sample ground.

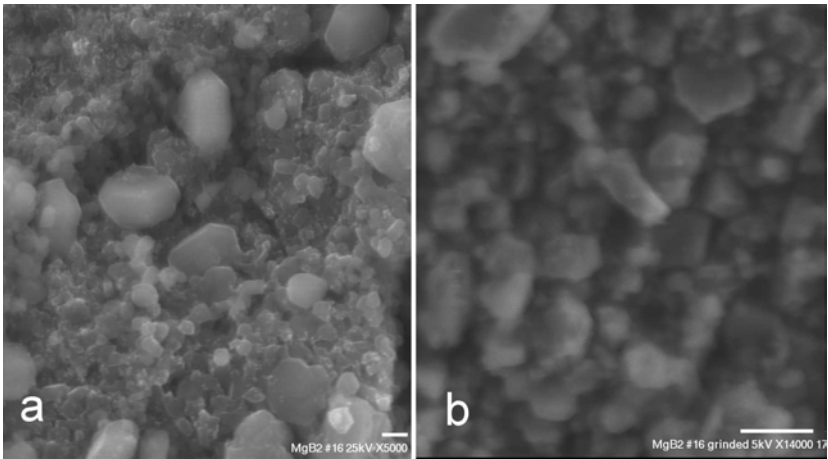


Fig. 2- SEM micrographs of (a) sintered and (b) ground un-HIPed sample.

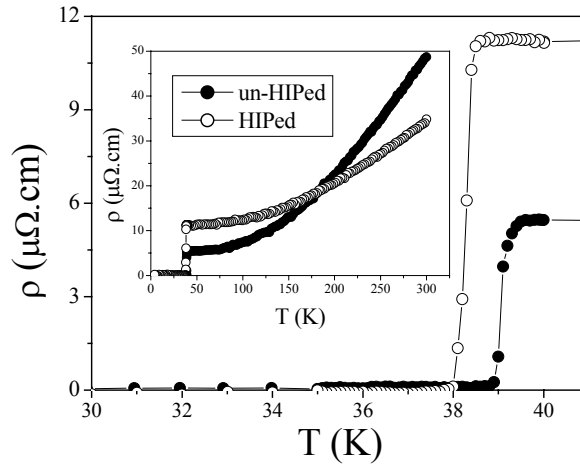


Fig. 3- Dc resistivity as a function of temperature for the un-HIPed and HIPed samples. The inset show an extended range of temperature.

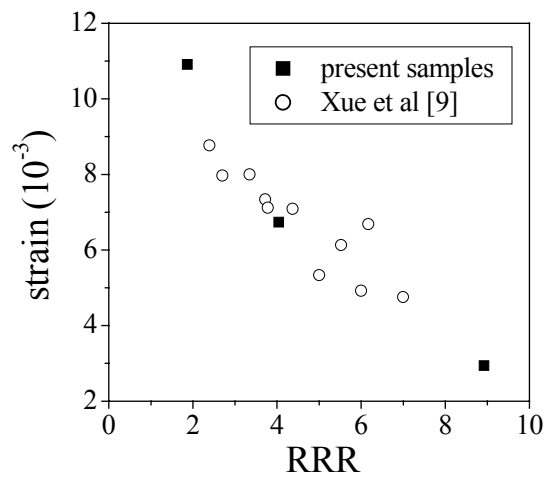


Fig. 4 - The strain vs. $RRR = \rho(297\text{ K})/\rho(40\text{ K})$ of the present samples reported in reference [11].

For comparison we show the results of Xue et al.⁹

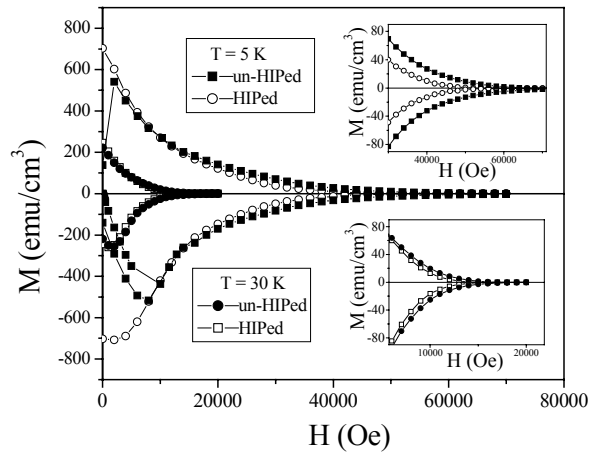


Fig. 5- Magnetization M as a function of magnetic field H at 5 and 30 K for the un-HIPed and HIPed samples. Upper inset: expanded view showing the onset of the reversible regime at 5 K. Lower inset: expanded view showing the onset of the reversible regime at 30 K.

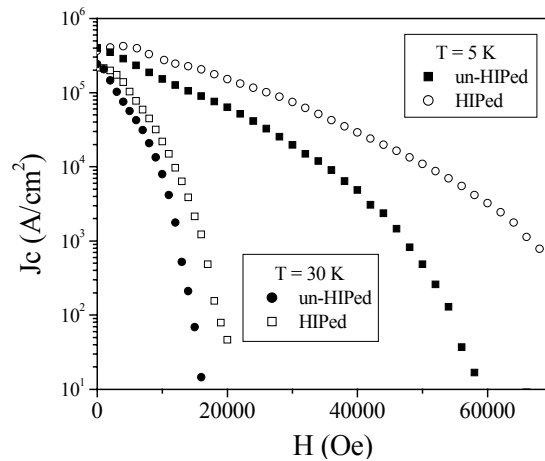


Fig. 6- Magnetization critical current density J_c as a function of magnetic field H for the un-HIPed and HIPed samples at 5 and 30 K. As discussed in the text, the J_c at 0 field is nearly the same for both samples, but the differences between the samples increases with field, and the drop in J_c at higher fields is remarkably faster in the un-HIPed sample than in the HIPed one

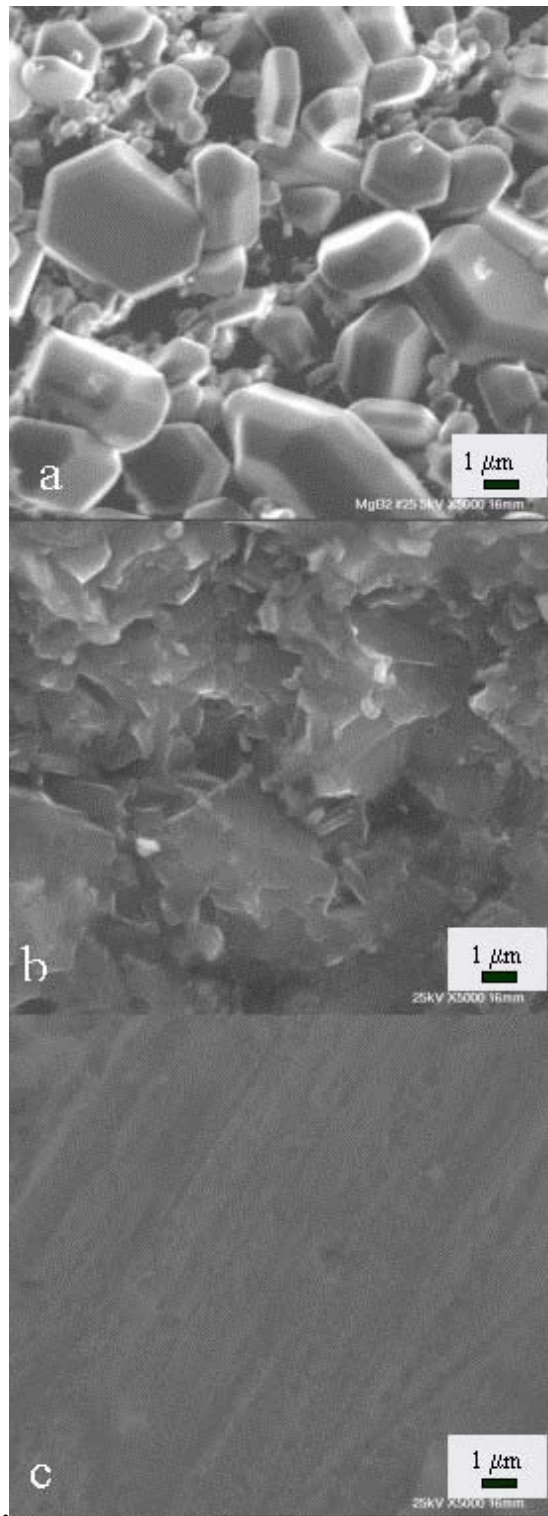


Fig. 7- SEM micrographs of MgB₂ samples: (a) surface of un-HIPed sample, (b) HIPed sample and (c) polished HIPed sample.

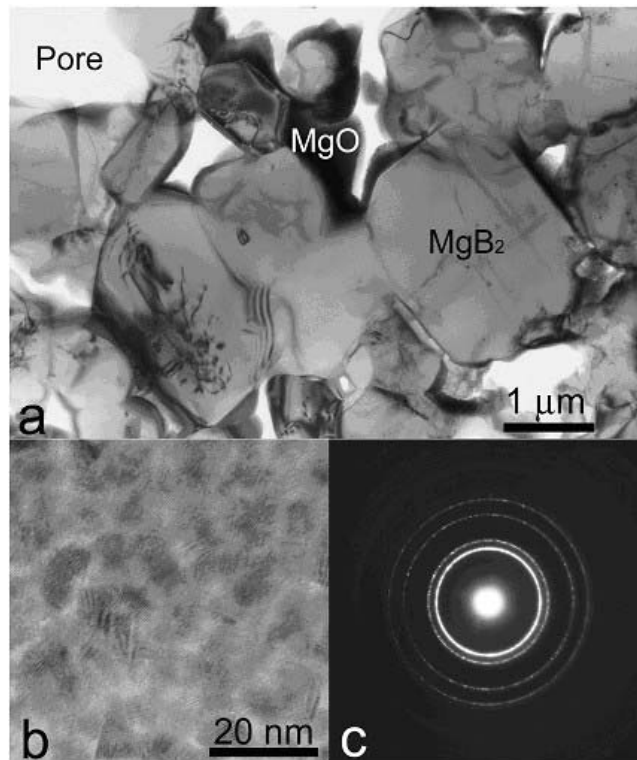


Fig. 8- (a) A bright-field image of the un-HIPed sample reveals poor connectivity among MgB₂ grains. Pores and MgO at the grain boundaries of MgB₂ are seen; (b) a magnified image of a MgO area showing the nanometer-sized grains characteristic of MgO; (c) electron diffraction pattern of MgO from one of these areas.

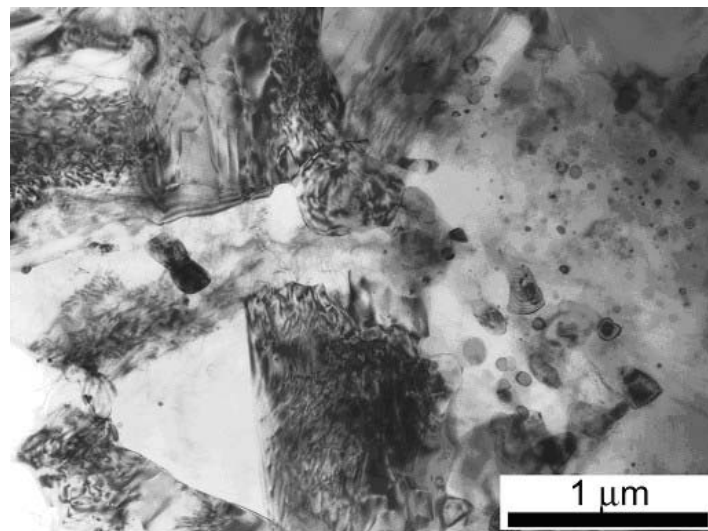


Fig. 9- A bright-field image of the HIPed sample shows that connectivity among the MgB₂ grains has been greatly improved. No pores are seen.

References

- ¹ J. Nagamatsu, N. Nakagawa, T. Muranaka, Y. Zenitani, and J. Akimitsu, *Nature (London)* **410**, 63 (2001).
- ² Y. Bugoslavsky, L. F. Cohen, G. K. Perkins, M. Polichetti, T. J. Tate, R. Gwilliam, A. D. Caplin, *Nature (London)* **11**, 561 (2001).
- ³ D. C. Larbalestier, L. D. Cooley, M. O. Rikel, A. A. Polyanskii, J. Jiang, S. Patnaik, X. Y. Cai, D. M. Feldmann, A. Gurevich, and A. A. Squitieri, *Nature (London)* **410**, 186 (2001).
- ⁴ T. C. Shields, K. Kawano, D. Holdom, and J. S. Abell, Preprint cond-mat/0107034 (2001).
- ⁵ L. Gozzelino, F. Laviano, D. Botta, A. Chiodoni, R. Gerbaldo, G. Ghigo, E. Mezzetti, G. Giunchi, S. Ceresara, G. Ripamonti, M. Poyer, Preprint cond-mat/0104069 (2001).
- ⁶ C. Buzea and T. Yamashita, Preprint cond-mat/0108265 (2001).
- ⁷ S. S. Indrakanti, V. F. Nesterenko, M. B. Maple, N. A. Frederick, W. M. Yuhasz, Shi Li, *Philos. Mag. Lett.* **81**, 849 (2001).
- ⁸ C.U. Jung, M.S. Park, W.N. Kang, M.S. Kim, S.Y. Lee, S.I. Lee, *Physica C* **353**, 162 (2001).
- ⁹ Y.Y. Xue, R. L. Meng, B. Lorenz, J. M. Meen, Y. Y. Sun, and C. W. Chu, Preprint cond-mat/0105478 (24 May 2001).
- ¹⁰ N. A. Frederick, Shi Li, M. B. Maple, V. F. Nesterenko, S. S. Indrakanti, *Physica C* **363**, 1 (2001).
- ¹¹ A. Serquis, Y. T. Zhu, E. J. Peterson, J. Y. Coulter, D. E. Peterson, and F. M. Mueller, *Appl. Phys. Lett.* **x**, x (2001).

-
- ¹² X. Z. Liao, A. Serquis, Y. T. Zhu, J. Y. Huang, J. O. Willis, D. E. Peterson, and F. M. Mueller, submitted.
- ¹³ P.C. Canfield, D.K. Finnemore, S.L. Bud'ko, J.E. Ostenson, G. Lapertot, C.E. Cunningham, C. Petrovic, Phys. Rev. Lett. **86**, 2423 (2001).
- ¹⁴ D.K. Finnemore, J.E. Ostenson, S.L. Bud'ko, G. Lapertot, P.C. Canfield, Phys. Rev. Lett. **86**, 2420 (2001).
- ¹⁵ Y. Takano, H. Takeya, H. Fujii, H. Kumakura, T. Hatano, K. Togano, H. Kito, H. Ihara, Appl. Phys. Lett. **78**, 2914 (2001).
- ¹⁶ C. Panagopoulos, B.D. Rainford, T. Xiang, C.A. Scott, M. Kambara, I.H. Inoue, Phys. Rev. B **64**, 4514 (2001).
- ¹⁷ J.R. Thompson, M. Paranthaman, D.K. Christen, K.D. Sorge, H.J. Kim, J.G. Ossandon, Supercond. Sci. Technol. **14**, L17 (2001).
- ¹⁸ N. Rogado, M.A. Hayward, K.A. Regan, Y. Wang, N.P. Ong, J. M. Rowell, and R. J. Cava, Preprint cond-mat/0107534 (2001).
- ¹⁹ S. Lee, H. Mori, T. Masui, Y. Eltsev, A. Yamamoto, and S. Tajima, J. Phys. Soc. Jpn. **27**, 54 (2001).
- ²⁰ C.P. Bean, Phys. Rev. Lett. **8**, 250 (1962).
- ²¹ S.X. Dou, X.L. Wang, J. Horvat, D. Milliken, A.H. Li, K. Konstantinov, E.W. Collings, M.D. Sumption, H.K. Liu, Physica C **361**, 79 (2001).